



# Establishing the Taxa and Functional profile of Microbiota implicated in West Nile Fever

Jemy Ratna Jovita<sup>1,2\*</sup>, Shylesh Murthy IA<sup>2</sup> and Preenon Bagchi<sup>3</sup>

<sup>1</sup>Padmashree Institute of Management and Sciences, Bengaluru, India.

\*E-mail: jemy2798@gmail.com

<sup>2</sup>Vasishth Academy of Advanced Studies and Research, Bengaluru, India.

<sup>3</sup>Institute of Biosciences and Technology, MGM University, Aurangabad, India

**Abstract:** West Nile fever causing microbiome is taken in this work. *Culex nigripalpus* mosquito is the causative factor for West Nile Virus. Using Metatranscriptomic sequencing, identified the taxa and functional profile of the microbiome is identified.

**Keywords:** West Nile fever, microbiome, Metatranscriptomics, taxonomy, functional profile, gene receptors, docking.

## 1. INTRODUCTION

West Nile fever is an infection caused by the West Nile virus, which is spread by mosquito, *Culex nigripalpus*. *Culex nigripalpus* is a primary vector for causing West Nile fever; they proliferate in the nutrient rich media and colonize in freshwater aquatic habitats. The microbiota of mosquitoes provides nutrition for the development and transmission of the pathogen [1, 2]. The virus replicates affecting the brain causing neuro-virulence, it turns to be neuroinvasive when it gains access to the central nervous system. The viral serine protease, NS2B-NS3 plays a crucial role in viral replication. The distribution of the virus is seen throughout Africa, the Middle East, southern Europe, western Russia, southwestern Asia, and Australia [3].

The Src family kinase c-Yes was recently reported to be important for maturation of West Nile virus particles. Individuals with West Nile fever recover within days to months. In acute flaccid paralysis individuals develop symptoms headache, fever, malaise, gastrointestinal upset, skin rash, and some patients have neck rigidity and changes in mental status [4].

## 2. MATERIALS AND METHODS

### Metatranscriptomic analysis

Next-generation sequencing (NGS) is an advanced version of non-Sanger-based sequencing technology that offers ultra-high throughput, scalability, and speed. Galaxy is an open source, web-based platform for next generation computational biomedical research [5]. Metatranscriptomics analysis enables understanding of how the microbiome responds to the environment by studying the functional analysis of genes expressed by the microbiome [6, 7].

Structure based drug designing technique is used here to build, display, simulate and analyze the molecular structure. Here we have used SWISS-MODEL tool [8] for modelling the proteins (gene receptors) responsible for West Nile fever CCR5, CLEC4M, IFITM2, IRF3. Selected models from homology modelling [9] output are docked with selected phytocompound from medicinal herbs.

Selection of phytocompounds was done using Lipinski rule for drug which is based on the ADME properties. Molecular docking [10] was done using Patchdock tool and best interacting phytocompounds with the gene receptors can be selected as ligands.

West Nile viruses' fastq sequences SRR10017187.1.1 and SRR10017187.1.2 were retrieved from SRA database.

Sequences' quality was checked using FASTQC [11]. MultiQC [12] was done to aggregate results from FASTQC analyses into a single report.

Sequences were trimmed using cutadapt.

FASTQC followed by MultiQC was re-run using the results of cutadapt.

Next, using SortMeRNA tool [13-17] any reads identified as rRNA in dataset was removed.

Next, using FASTQ INTERLACE tool [18] paired end FASTQ reads from two separate files were joined.

MetaPhlAn tool [19] was used for profiling the composition of microbial communities (Bacteria, Archaea and Eukaryotes) from our microbiota.

Krona tool [20, 21] was used to visualize the results of a metagenomic profiling as a zoomable pie chart and GraPhlAn tool [22] for visualizing high-quality circular representations of taxonomic and phylogenetic trees.

Further, HUMAnN [23] pipeline was used for efficiently and accurately profiling the presence/absence and abundance of microbial pathways in our microbiota.

### 3. RESULTS AND DISCUSSION

Metagenome, having accession number SRR10017187, for West Nile virus was downloaded from SRA database.

As, per **Per base sequence quality** results of FASTQC and MultiQC, the sequence quality is not good hence we go ahead with trimming the sequence.

CUTADAPT tool [24] is used for trimming. It finds and removes adapter sequences, primers, poly-A tails, and other types of unwanted sequence from our data. It searches for the adapter in all reads and removes it when it finds it. Further, sequence quality of the cutadapt output is checked using FASTQC and MultiQC and it is found within the range.

SortMeRNA tool removes any reads identified as rRNA from our dataset. Fastq Interlace tool joins paired end FASTQ reads from two separate files. Taxonomic profiling [25] was done using MetaPhlAn tool.

The output is visualized using Krona and Graphlan.



Fig. 1: Generation, personalization and annotation of tree: Tree in PhyloXML

Table 1: MetaPhlAn: Predicted taxon relative abundances at each taxonomic levels

kingdom	kingdom_id	phylum	class	order	family	family_id	genus	genus_id	species	species_id	strains	strains_id
Viruses	10239					100.0						
Viruses	10239	Viruses unclassified					100.0					
Viruses	10239	Viruses unclassified	Viruses unclassified					100.0				
Viruses	10239	Viruses unclassified	Viruses unclassified	Viruses unclassified					100.0			
Viruses	10239	Viruses unclassified	Viruses unclassified	Viruses unclassified	Flaviviridae	11050				100.0		
Viruses	10239	Viruses unclassified	Viruses unclassified	Viruses unclassified	Flaviviridae	11050	Flavivirus	11051			100.0	
Viruses	10239	Viruses unclassified	Viruses unclassified	Viruses unclassified	Flaviviridae	11050	Flavivirus	11051	West Nile virus	11082		100.0

After generation of taxonomy, we move to functional information of our microbiome. Functional information of the above microbiome community [28] was done using HUMAnN pipeline.

# Gene Family	humann_Abundance-RELAB
UNMAPPED	0.888769
UniRef90_D9MXB1	0.0073362
UniRef90_D9MXB1 unclassified	0.0073362
UniRef90_UPI0001DD3770	0.00495637
UniRef90_UPI0001DD3770 unclassified	0.00495637
UniRef90_A0A1B1WW31	0.00484378
UniRef90_A0A1B1WW31 unclassified	0.00484378
UniRef90_B9DF73	0.00459488
UniRef90_B9DF73 unclassified	0.00459488
UniRef90_A0A067ZQ74	0.00422115
UniRef90_A0A067ZQ74 unclassified	0.00422115
UniRef90_A0A077EZ14	0.00417222
UniRef90_A0A077EZ14 unclassified	0.00417222
UniRef90_A0A067ZS80	0.00390475

UniRef90_A0A067ZS80 unclassified	0.00390475
UniRef90_UPI0003F054D7	0.00376104
UniRef90_UPI0003F054D7 unclassified	0.00376104
UniRef90_F1BA45	0.0036982
UniRef90_F1BA45 unclassified	0.0036982
UniRef90_A0A1X3CH90	0.00318336
UniRef90_A0A1X3CH90 unclassified	0.00318336
UniRef90_UPI000D0C92C0	0.00302072
UniRef90_UPI000D0C92C0 unclassified	0.00302072
UniRef90_K9L2G3	0.00265002
UniRef90_K9L2G3 unclassified	0.00265002
UniRef90_A0A1B1WWN4	0.00258533
UniRef90_A0A1B1WWN4 unclassified	0.00258533
UniRef90_K7ET80	0.00256502
UniRef90_K7ET80 unclassified	0.00256502

UniRef90_Q91CD9	0.00251161
UniRef90_Q91CD9 unclassified	0.00251161
UniRef90_UPI00018E17CF	0.00240202
UniRef90_UPI00018E17CF unclassified	0.00240202
UniRef90_G7PXF9	0.00234066
UniRef90_G7PXF9 unclassified	0.00234066
UniRef90_F6Z663	0.00218081
UniRef90_F6Z663 unclassified	0.00218081
UniRef90_G7MFM1	0.00215974
UniRef90_G7MFM1 unclassified	0.00215974
UniRef90_A0A2K6NB76	0.0020891
UniRef90_A0A2K6NB76 unclassified	0.0020891
UniRef90_UPI000181CCFE	0.00203554
UniRef90_UPI000181CCFE unclassified	0.00203554
UniRef90_C9WPK8	0.00195453
UniRef90_C9WPK8 unclassified	0.00195453
UniRef90_P14335	0.00180304
UniRef90_P14335 unclassified	0.00180304
UniRef90_F7HJ82	0.00180269
UniRef90_F7HJ82 unclassified	0.00180269
UniRef90_A0A0D3MDX0	0.00160595
UniRef90_A0A0D3MDX0 unclassified	0.00160595
UniRef90_UPI0000E69E2F	0.00153697
UniRef90_UPI0000E69E2F unclassified	0.00153697
UniRef90_I3VPR6	0.00149368
UniRef90_I3VPR6 unclassified	0.00149368
UniRef90_G8E0A9	0.00146336
UniRef90_G8E0A9 unclassified	0.00146336
UniRef90_D3X888	0.0013421
UniRef90_D3X888 unclassified	0.0013421
UniRef90_UPI00003BECBC	0.00130469
UniRef90_UPI00003BECBC unclassified	0.00130469
UniRef90_UPI0002C39258	0.00127138
UniRef90_UPI0002C39258 unclassified	0.00127138
UniRef90_Q6VXX6	0.00120319
UniRef90_Q6VXX6 unclassified	0.00120319
UniRef90_D3X8F1	0.0011535
UniRef90_D3X8F1 unclassified	0.0011535
UniRef90_A0A1S6WNB4	0.00110115
UniRef90_A0A1S6WNB4 unclassified	0.00110115
UniRef90_D3X8F7	0.00102768
UniRef90_D3X8F7 unclassified	0.00102768
UniRef90_D3X8D8	0.000998791
UniRef90_D3X8D8 unclassified	0.000998791
UniRef90_Q91KP3	0.000989086
UniRef90_Q91KP3 unclassified	0.000989086
UniRef90_D9IFF5	0.000952321
UniRef90_D9IFF5 unclassified	0.000952321
UniRef90_F7EY45	0.000912381
UniRef90_F7EY45 unclassified	0.000912381
UniRef90_D5K1B9	0.00090469
UniRef90_D5K1B9 unclassified	0.00090469
UniRef90_Q67428	0.000861045
UniRef90_Q67428 unclassified	0.000861045
UniRef90_Q91AB0	0.000854561
UniRef90_Q91AB0 unclassified	0.000854561
UniRef90_D3X875	0.000850089
UniRef90_D3X875 unclassified	0.000850089

UniRef90_A0A2K5WQL4	0.000795493
UniRef90_A0A2K5WQL4 unclassified	0.000795493
UniRef90_B1P6F1	0.000689513
UniRef90_B1P6F1 unclassified	0.000689513
UniRef90_P29984	0.000618302
UniRef90_P29984 unclassified	0.000618302
UniRef90_A0A0B5H4C4	0.000582165
UniRef90_A0A0B5H4C4 unclassified	0.000582165
UniRef90_Q6YFU6	0.00051542
UniRef90_Q6YFU6 unclassified	0.00051542
UniRef90_A0A0P0RST2	0.000505187
UniRef90_A0A0P0RST2 unclassified	0.000505187
UniRef90_A0A0D5CWD5	0.000489091
UniRef90_A0A0D5CWD5 unclassified	0.000489091
UniRef90_A0A068AXW2	0.000463204
UniRef90_A0A068AXW2 unclassified	0.000463204
UniRef90_A0A1X3CWX3	0.000451315
UniRef90_A0A1X3CWX3 unclassified	0.000451315
UniRef90_I1TEC3	0.000443267
UniRef90_I1TEC3 unclassified	0.000443267
UniRef90_A0A229QXW6	0.000390111
UniRef90_A0A229QXW6 unclassified	0.000390111
UniRef90_UPI0000485C0B	0.000373856
UniRef90_UPI0000485C0B unclassified	0.000373856
UniRef90_Q6VXX7	0.000367549
UniRef90_Q6VXX7 unclassified	0.000367549
UniRef90_H2NBX3	0.000356109
UniRef90_H2NBX3 unclassified	0.000356109
UniRef90_UPI000642CDD8	0.000349761
UniRef90_UPI000642CDD8 unclassified	0.000349761
UniRef90_I3N2P9	0.000333919
UniRef90_I3N2P9 unclassified	0.000333919
UniRef90_D9IFG5	0.000299914
UniRef90_D9IFG5 unclassified	0.000299914
UniRef90_D3X874	0.000283626
UniRef90_D3X874 unclassified	0.000283626
UniRef90_Q9DP92	0.000282183
UniRef90_Q9DP92 unclassified	0.000282183
UniRef90_D3X8B2	0.000279068
UniRef90_D3X8B2 unclassified	0.000279068
UniRef90_A0A075FC35	0.000211602
UniRef90_A0A075FC35 unclassified	0.000211602
UniRef90_B7U2U9	0.000200363
UniRef90_B7U2U9 unclassified	0.000200363
UniRef90_C9WPM0	0.000194638
UniRef90_C9WPM0 unclassified	0.000194638
UniRef90_A0A0P7UTC2	0.000191691
UniRef90_A0A0P7UTC2 unclassified	0.000191691
UniRef90_F7FBV8	0.000191691
UniRef90_F7FBV8 unclassified	0.000191691
UniRef90_G3SQL6	0.000191691
UniRef90_G3SQL6 unclassified	0.000191691
UniRef90_H3BYH5	0.000191691
UniRef90_H3BYH5 unclassified	0.000191691
UniRef90_P60866	0.000191691
UniRef90_P60866 unclassified	0.000191691
UniRef90_D3X8C7	0.000186455
UniRef90_D3X8C7 unclassified	0.000186455

UniRef90_A0A2K6EGR5	0.000170037
UniRef90_A0A2K6EGR5 unclassified	0.000170037
UniRef90_A0A0B7JKQ7	0.000166418
UniRef90_A0A0B7JKQ7 unclassified	0.000166418
UniRef90_UPI0005215E94	0.000165638
UniRef90_UPI0005215E94 unclassified	0.000165638
UniRef90_G3I2D3	0.00016095
UniRef90_G3I2D3 unclassified	0.00016095
UniRef90_A0A2I0MVY6	0.000152329
UniRef90_A0A2I0MVY6 unclassified	0.000152329
UniRef90_L9LBB7	0.000143369
UniRef90_L9LBB7 unclassified	0.000143369
UniRef90_UPI0006B0C551	0.000133289
UniRef90_UPI0006B0C551 unclassified	0.000133289
UniRef90_A0A091DCD6	0.000130236
UniRef90_A0A091DCD6 unclassified	0.000130236

UniRef90_UPI000D3231B4	0.00012363
UniRef90_UPI000D3231B4 unclassified	0.00012363
UniRef90_UPI000359548B	0.000119308
UniRef90_UPI000359548B unclassified	0.000119308
UniRef90_UPI00051F13F9	0.000116856
UniRef90_UPI00051F13F9 unclassified	0.000116856
UniRef90_UPI0005216B30	0.000112244
UniRef90_UPI0005216B30 unclassified	0.000112244
UniRef90_K7P5A3	0.000108977
UniRef90_K7P5A3 unclassified	0.000108977
UniRef90_L5JT11	8.00319e-05
UniRef90_L5JT11 unclassified	8.00319e-05
UniRef90_Q6VYH3	7.08503e-05
UniRef90_Q6VYH3 unclassified	7.08503e-05
UniRef90_A0A2U3XJL7	5.7032e-05
UniRef90_A0A2U3XJL7 unclassified	5.7032e-05

Next, from the gene family information, we obtain the functional information of our microbiome using Superfamily server. The Functional information of 1<sup>st</sup> five families from Normalized gene families as detected by Superfamily (HMM library and genome assignments server) is given below.

<p><b>Strong hits</b></p> <p>Sequence: <a href="#">G9R4D3</a></p> <p>Domain Number 1: Region: 296-430</p> <p>Classification Level Classification E-value</p> <p>Superfamily <a href="#">P-loop containing nucleoside triphosphate hydrolases</a> 3.45e-55</p> <p>Family <a href="#">RNA helicase</a> 0.00000358</p> <p>Further Details: <a href="#">Family Details</a> <a href="#">Alignments</a> <a href="#">Genome Assignments</a> <a href="#">Domain Comparisons</a></p> <p>Domain Number 2: Region: 3-284</p> <p>Classification Level Classification E-value</p> <p>Superfamily <a href="#">P-loop containing nucleoside triphosphate hydrolases</a> 6.2e-40</p> <p>Family <a href="#">RNA helicase</a> 0.0000000421</p> <p>Further Details: <a href="#">Family Details</a> <a href="#">Alignments</a> <a href="#">Genome Assignments</a> <a href="#">Domain Comparisons</a></p>	<p><b>Protein sequence</b></p> <p>External ID: <a href="#">UniProt</a></p> <p>Sequence length: 352</p> <p>Comment: <a href="#">UniProt</a></p> <p>Download: <a href="#">FASTA</a> <a href="#">FASTQ</a> <a href="#">SRA</a></p>
<p>UniRef90_D9MXB1   Abundance-0.0073362</p>	
<p><b>Strong hits</b></p> <p>Sequence: <a href="#">AGA1B1WW31</a></p> <p>Domain Number 1: Region: 291-590</p> <p>Classification Level Classification E-value</p> <p>Superfamily <a href="#">Viral glycoprotein, central acid disintegration domains</a> 1.26e-126</p> <p>Family <a href="#">Viral glycoprotein, central acid disintegration domains</a> 0.0000000834</p> <p>Further Details: <a href="#">Family Details</a> <a href="#">Alignments</a> <a href="#">Genome Assignments</a> <a href="#">Domain Comparisons</a></p> <p>Domain Number 2: Region: 1090-2124</p> <p>Classification Level Classification E-value</p> <p>Superfamily <a href="#">P-loop containing nucleoside triphosphate hydrolases</a> 1.06e-34</p> <p>Family <a href="#">RNA helicase</a> 0.00000358</p> <p>Further Details: <a href="#">Family Details</a> <a href="#">Alignments</a> <a href="#">Genome Assignments</a> <a href="#">Domain Comparisons</a></p> <p>Domain Number 3: Region: 382-996</p> <p>Classification Level Classification E-value</p> <p>Superfamily <a href="#">E set domains</a> 4.48e-44</p> <p>Family <a href="#">Class II viral fusion proteins C-terminal domain</a> 0.000000784</p> <p>Further Details: <a href="#">Family Details</a> <a href="#">Alignments</a> <a href="#">Genome Assignments</a> <a href="#">Domain Comparisons</a></p> <p>Domain Number 4: Region: 1687-1979</p> <p>Classification Level Classification E-value</p> <p>Superfamily <a href="#">P-loop containing nucleoside triphosphate hydrolases</a> 1.93e-40</p> <p>Family <a href="#">RNA helicase</a> 0.0000000317</p> <p>Further Details: <a href="#">Family Details</a> <a href="#">Alignments</a> <a href="#">Genome Assignments</a> <a href="#">Domain Comparisons</a></p> <p>Domain Number 5: Region: 1510-1676</p> <p>Classification Level Classification E-value</p> <p>Superfamily <a href="#">Trypsin-like serine proteases</a> 9.27e-36</p> <p>Family <a href="#">Viral proteases</a> 0.000000259</p> <p>Further Details: <a href="#">Family Details</a> <a href="#">Alignments</a> <a href="#">Genome Assignments</a> <a href="#">Domain Comparisons</a></p> <p>Domain Number 6: Region: 22-99</p> <p>Classification Level Classification E-value</p> <p>Superfamily <a href="#">Flavivirus capsid protein C</a> 1.44e-31</p> <p>Family <a href="#">Flavivirus capsid protein C</a> 0.0000192</p> <p>Further Details: <a href="#">Family Details</a> <a href="#">Alignments</a> <a href="#">Genome Assignments</a> <a href="#">Domain Comparisons</a></p>	<p><b>Protein sequence</b></p> <p>Sequence length: 2584</p> <p>Comment: (tr A0A1B1WW31 A0A1B1WW31_WNV) Genome polyprotein {ECO:0000256 SAAS:SAAS00368684} OX=11082 OS=West Nile virus (WNV). GN=MZ11_60591gpGP3 OC=Flaviviridae; Flavivirus; Japanese encephalitis virus group. OH=7158,8782,9606,34610,34627,34630,5352 7,308735,308737</p>
<p>UniRef90_A0A1B1WW31   Abundance-0.00484378</p>	

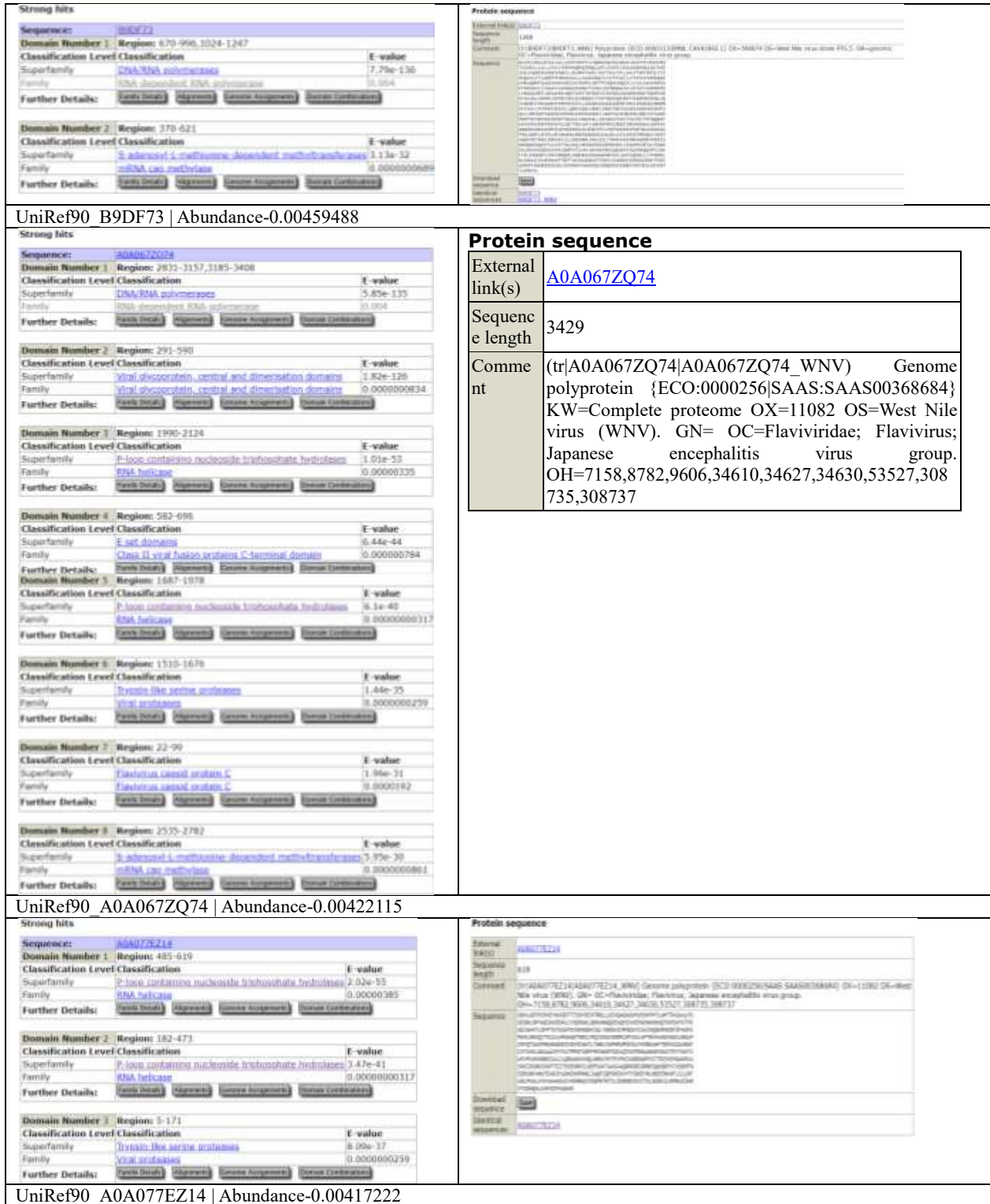


Fig. 2: Functional information of 1<sup>st</sup> five gene families as detected by Superfamily server [26]

**CONCLUSION**

The taxonomy information of West Nile fever microbiome are identified. The functional

information of the microbiome was identified using Superfamily database. This family information will be useful for further drug designing studies.

## REFERENCE

1. Duguma, D., Hall, M. W., Smartt, C. T., Debboun, M., & Neufeld, J. D. (2019). Microbiota variations in *Culex nigripalpus* disease vector mosquito of West Nile virus and Saint Louis Encephalitis from different geographic origins. *PeerJ*, 6, e6168.
2. Ezgimen, M., Lai, H., Mueller, N. H., Lee, K., Cuny, G., Ostrov, D. A., & Padmanabhan, R. (2012). Characterization of the 8-hydroxyquinoline scaffold for inhibitors of West Nile virus serine protease. *Antiviral research*, 94(1), 18-24.
3. Petersen, L. R., Brault, A. C., & Nasci, R. S. (2013). West Nile virus: review of the literature. *Jama*, 310(3), 308-315.
4. Kramer, L. D., Li, J., & Shi, P. Y. (2007). West Nile virus. *The Lancet Neurology*, 6(2), 171-181.
5. Blankenberg, D., & Hillman-Jackson, J. (2014). Analysis of next-generation sequencing data using Galaxy. In *Stem cell transcriptional networks* (pp. 21-43). Humana Press, New York, NY.
6. Bashiardes S, Zilberman-Schapira G, and Elinav E, (2016), Use of Metatranscriptomics in Microbiome Research, *Bioinform Biol Insights.* ; 10: 19–25.
7. Handelsman J, (2004), Metagenomics: Application of Genomics to Uncultured Microorganisms, *Microbiol Mol Biol Rev.* 68(4): 669–685.
8. Waterhouse A, Bertoni M, Bienert S, Studer G, Tauriello G, Gumienny R, Heer FT, A P de Beer T, Rempfer C, Bordoli L, Lepore R and Schwede T, (2018), SWISS-MODEL: homology modelling of protein structures and complexes, *Nucleic Acids Res.*; 46(Web Server issue): W296–W303.
9. Vyas VK, Ukawala RD, Ghate M, and Chintha C (2012), Homology Modeling a Fast Tool for Drug Discovery: Current Perspectives, *Indian J Pharm Sci.*74(1): 1–17.
10. Morris GM, Lim-Wilby M, (2008), Molecular docking, *Methods Mol Biol*, 443:365-82.
11. Andrews, S. (n.d.). FastQC A Quality Control tool for High Throughput Sequence Data. Retrieved from <http://www.bioinformatics.babraham.ac.uk/projects/fastqc/>
12. Ewels, P., Magnusson, M., Lundin, S., & K oller, M. (2016). MultiQC: summarize analysis results for multiple tools and samples in a single report. *Bioinformatics*, 32(19), 3047–3048. <https://doi.org/10.1093/bioinformatics/btw354>
13. Kopylova, E., No e, L., & Touzet, H. (2012). SortMeRNA: fast and accurate filtering of ribosomal RNAs in metatranscriptomic data. *Bioinformatics*, 28(24), 3211–3217. <https://doi.org/10.1093/bioinformatics/bts611>
14. Quast, C., Pruesse, E., Yilmaz, P., Gerken, J., Schweer, T., Yarza, P., ... Gl ockner, F. O. (2012). The SILVA ribosomal RNA gene database project: improved data processing and web-based tools. *Nucleic Acids Research*, 41(D1), D590–D596. <https://doi.org/10.1093/nar/gks1219>
15. Burge, S. W., Daub, J., Eberhardt, R., Tate, J., Barquist, L., Nawrocki, E. P., ... Bateman, A. (2012). Rfam 11.0: 10 years of RNA families. *Nucleic Acids Research*, 41(D1), D226–D232. <https://doi.org/10.1093/nar/gks1005>
16. Edgar, R. C. (2010). Search and clustering orders of magnitude faster than BLAST. *Bioinformatics*, 26(19), 2460–2461. <https://doi.org/10.1093/bioinformatics/btq461>
17. Loman, N. J., Misra, R. V., Dallman, T. J., Constantinidou, C., Gharbia, S. E., Wain, J., & Pallen, M. J. (2012). Performance comparison of benchtop high-throughput sequencing platforms. *Nature Biotechnology*, 30(5), 434–439. <https://doi.org/10.1038/nbt.2198>
18. Blankenberg, D., Gordon, A., Von Kuster, G., Coraor, N., Taylor, J., & and, A. N. (2010). Manipulation of FASTQ data with Galaxy. *Bioinformatics*, 26(14), 1783–1785. <https://doi.org/10.1093/bioinformatics/btq281>
19. Beghini, F., McIver, L. J., Blanco-Miguez, A., Dubois, L., Asnicar, F., Maharjan, S., ... Segata, N. (2021). Integrating taxonomic, functional, and strain-level profiling of diverse microbial communities with bioBakery 3. *ELife*, 10. <https://doi.org/10.7554/elife.65088>
20. Ondov, B. D., Bergman, N. H., & Phillippy, A. M. (2011). Interactive metagenomic visualization in a Web browser. *BMC Bioinformatics*, 12(1). <https://doi.org/10.1186/1471-2105-12-385>

21. Cuccuru, G., Orsini, M., Pinna, A., Sbardellati, A., Soranzo, N., Travaglione, A., ... Fotia, G. (2014). Orione, a web-based framework for NGS analysis in microbiology. *Bioinformatics*, 30(13), 1928–1929. <https://doi.org/10.1093/bioinformatics/btu135>
22. Asnicar, F., Weingart, G., Tickle, T. L., Huttenhower, C., & Segata, N. (2015). Compact graphical representation of phylogenetic data and metadata with GraPhlAn. *PeerJ*, 3, e1029. <https://doi.org/10.7717/peerj.1029>
23. Abubucker, S., Segata, N., Goll, J., Schubert, A. M., Izard, J., Cantarel, B. L., ... Huttenhower, C. (2012). Metabolic Reconstruction for Metagenomic Data and Its Application to the Human Microbiome. *PLoS Computational Biology*, 8(6), e1002358. <https://doi.org/10.1371/journal.pcbi.1002358>
24. Martin, M. (2011). Cutadapt removes adapter sequences from high-throughput sequencing reads. *EMBnet.Journal*, 17(1), 10. <https://doi.org/10.14806/ej.17.1.200>
25. Jagtap P, Mehta S, Sajulga R, Batut B, Leith E, Kumar P, Hiltmann S, 2021 Metatranscriptomics analysis using microbiome RNA-seq data (Galaxy Training Materials).
26. Gough, J., Karplus, K., Hughey, R. and Chothia, C. (2001). Assignment of Homology to Genome Sequences using a Library of Hidden Markov Models that Represent all Proteins of Known Structure. *J. Mol. Biol.*, 313(4), 903-919

**Open Access** This chapter is licensed under the terms of the Creative Commons Attribution-NonCommercial 4.0 International License (<http://creativecommons.org/licenses/by-nc/4.0/>), which permits any noncommercial use, sharing, adaptation, distribution and reproduction in any medium or format, as long as you give appropriate credit to the original author(s) and the source, provide a link to the Creative Commons license and indicate if changes were made.

The images or other third party material in this chapter are included in the chapter's Creative Commons license, unless indicated otherwise in a credit line to the material. If material is not included in the chapter's Creative Commons license and your intended use is not permitted by statutory regulation or exceeds the permitted use, you will need to obtain permission directly from the copyright holder.

